Mendeleev Communications

Mendeleev Commun., 2025, **35**, 573–576

Towards stable wide-bandgap perovskite absorbers: controlling light-induced halide phase segregation in $CsPbI_2Br$ through partial lead substitution

Marina I. Ustinova,[a,b] **Gennady V. Shilov,**[a] **Denis V. Korchagin,**[a] **Pavel A. Troshin,**[c,a]
Sergey M. Aldoshin[a] **and Lyubov A. Frolova***[a]

[a] *Federal Research Center of Problems of Chemical Physics and Medicinal Chemistry, Russian Academy of Sciences, 142432 Chernogolovka, Moscow Region, Russian Federation. E-mail: lyuanfro@gmail.com*
[b] *Centre for Hybrid and Organic Solar Energy, Department of Electronic Engineering, University of Rome Tor Vergata, 00133 Rome, Italy*
[c] *Zhengzhou Research Institute, Harbin Institute of Technology, 450003 Zhengzhou, China*

DOI: 10.71267/mencom.7698

The photostability of $CsPb_{0.95}M_{0.1/n}I_2Br$ films modified with 30 different substituent M^{n+} cations was systematically investigated. It was shown for the first time that light-induced halide phase segregation in $CsPbI_2Br$ perovskite films could be completely suppressed by partial replacement of Pb^{2+} with rationally selected cations: Sr^{2+}, Sn^{2+}, In^{3+} and Bi^{3+}. The obtained results open the door for the development of photostable wide-bandgap perovskite semiconductors required for high-efficiency tandem solar cells.

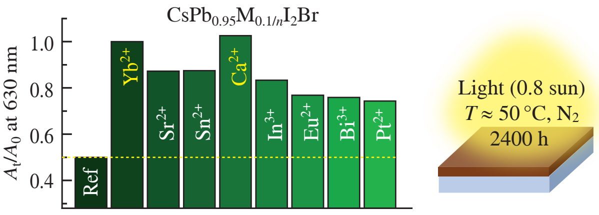

Keywords: perovskite solar cells, $CsPbI_2Br$, all-inorganic perovskite absorber, phase stability, photostability, partial lead substitution, halide phase segregation, long-term stability.

All-inorganic perovskite materials like $CsPbX_3$ (X = I, Br) attract attention due to their chemical robustness and optoelectronic properties, which enable high power conversion efficiency (PCE) in solar cells.[1–3] The black phases of $CsPbI_3$, which are cubic ($Pm\bar{3}m$) α, tetragonal ($P4/mbm$) β and orthorhombic ($Pbnm$) γ polymorphs, are characterized by the narrowest bandgap (1.72 eV) among the all-inorganic lead halide perovskites and, at the same time, thermodynamic instability at room temperature, which manifests itself in the transformation to the non-photoactive yellow δ-phase (2.82 eV).[4–6] Organic modifiers are often used to improve the phase stability of $CsPbI_3$, but such light-absorbing materials, strictly speaking, can no longer be called all-inorganic.[7,8] Partial substitution of I with Br stabilizes the perovskite phase in $CsPbI_{3-x}Br_x$, with $CsPbI_2Br$ providing an optimal balance of bandgap (1.92 eV) and stability for optoelectronic applications including tandem solar cells.[9–13] However, $CsPbI_2Br$ exhibits light-induced halide segregation, forming both Br-rich and I-rich domains.[14] To address this issue, we previously proposed using non-stoichiometric compositions with excess CsBr to passivate grain boundaries.[15] Alternatively, the resistance of $CsPbI_2Br$ to light-induced halide phase segregation could be improved by adding organic passivating molecules such as crown ethers, ammonium salts, amino acids, *etc.*[16–19] These strategies achieved PCEs of 14–17% but compromise the thermal and chemical stability of all-inorganic perovskites, limiting operational stability for tandem applications based on Si or CIGS technologies.[10–13]

Alternative approaches such as B-site modification (partial Pb substitution) have proven effective. We were among the first to apply this strategy to modify the properties of $MAPbI_3$ perovskite[20] and enhance the phase stability of $CsPbI_3$ perovskite,[21] recently publishing a comprehensive study on the effects of Pb^{2+} substitution in lead halide perovskites.[22] Recent studies show that the addition of $Ln(OTf)_3$ (Ln = Nd, Eu, Dy and Tm) to $CsPbI_2Br$ boosts the PCE (>15%) and stability by passivating halide vacancies.[23] Substitution with Zr^{4+} further enhances the efficiency (16.6%),[24] while other cations (*e.g.*, Ba^{2+}, Sr^{2+}, Mn^{2+}, Eu^{3+}, *etc.*) also improve the performance.[25–28]

Despite all the progress made in this particular field, a comprehensive understanding of the relationships between the properties of the introduced substituent cations and the effects produced on the device efficiency and stability is essentially lacking. In this work, we attempted to fill this gap and carried out a systematic study of the partial substitution of Pb^{2+} in $CsPbI_2Br$ with a large number of metal cations. The main objective of this work was to elucidate the influence of the modifying cations on the photostability of all-inorganic perovskite films, in particular on the occurrence of light-induced segregation of the halide phase.

Based on previous studies of lead substitution in $CsPbI_3$ and $MAPbI_3$,[21,22] we considered 5% substitution level in $CsPbI_2Br$ to

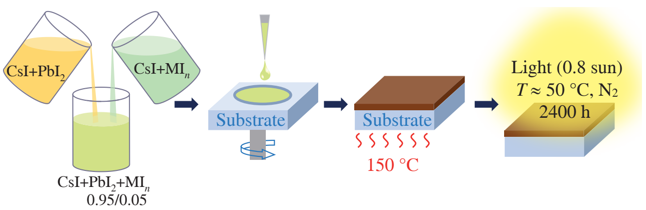

Figure 1 Experimental procedures for sample preparation and degradation testing.

be optimal to clearly observe the effect of each introduced cation. The sample preparation procedure† and degradation test conditions‡ are shown in Figure 1.

The reference $CsPbI_2Br$ films showed a spectral pattern very characteristic of light-induced segregation of the halide phase [Figure 2(*a*)]. In particular, the absorption band edge demonstrated a gradual bathochromic shift after 150–200 h of illumination, indicating the formation of an iodide-rich phase with a smaller band gap.

This process occurred during the first 1000–1500 h, and after 2000 h of aging, the band position shifted back to shorter wavelengths, while the spectral intensity in the range of 450–650 nm reduced dramatically. The observed changes are consistent with the initial formation of a narrow-bandgap black phase of $CsPbI_3$, which is thermodynamically unstable and undergoes a transformation to the yellow δ-phase, accompanied by a hypsochromic shift of the absorption band and severe spectral bleaching, since δ-$CsPbI_3$ absorbs only below 450 nm.[21] Analysis of the absorption spectra in Tauc coordinates suggests that the bandgap of the $CsPbI_2Br$ films decreased from 1.90 to 1.78 eV due to the formation of an I-rich phase [Figure S1(*a*), see Online Supplementary Materials]. Analysis of XRD patterns of films aged for 2400 h revealed the presence of dominant peaks of δ-$CsPbI_3$ and the perovskite phase of $CsPbBr_3$, indicating virtually complete segregation of bromide and iodide anions [Figure 2(*f*)]. The parent $CsPbI_2Br$ phase was not very clearly visible in the XRD patterns, most likely due to its strong amorphization.

The aging behavior of the films modified by partial substitution of Pb^{2+} differed quite significantly. Thus, among the series of samples loaded with alkaline earth metal cations, $CsPb_{0.95}Mg_{0.05}I_2Br$ and $CsPb_{0.95}Ca_{0.05}I_2Br$ demonstrated even faster light-induced degradation than the reference $CsPbI_2Br$ films, as evidenced by the massive bathochromic spectral shifts due to the accumulation of the I-rich phase [Figure 2(*c*),(*e*)]. XRD data confirmed that both Mg- and Ca-containing perovskite films were completely degraded after 2400 h of light exposure [Figure 2(*d*),(*f*)]. On the contrary, $CsPb_{0.95}Sr_{0.05}I_2Br$ films were found to be fairly stable and did not exhibit any significant spectral changes upon light exposure [Figure 2(*g*)]. The XRD patterns of the $CsPb_{0.95}Sr_{0.05}I_2Br$ films subjected to 2400 h of light soaking showed no signs of degradation [Figure 2(*h*)], indicating the remarkable photostability of the material with this composition. Thus, modification of $CsPbI_2Br$ with Sr^{2+} cations effectively suppressed the light-induced segregation of the halide phase. Compared with Sr^{2+}, the introduction of Ba^{2+} cations did not result in the same strong stabilization of the resulting perovskite films [Figure 2(*i*)]. Furthermore, the XRD data reveal complete degradation of the $CsPb_{0.95}Ba_{0.05}I_2Br$ films after 2400 h of light exposure [Figure 2(*j*)].

The obtained results indicate that Sr^{2+} is unique among alkaline earth metal cations in suppressing light-induced halide phase segregation in modified perovskite films. The bandgap of the $CsPb_{0.95}Sr_{0.05}I_2Br$ films was found to be significantly smaller than that of $CsPbI_2Br$ [Figure S1(*d*)], suggesting that the incorporation of Sr^{2+} has a strong effect on the optoelectronic properties and band structure of the perovskite semiconductor. Note that the Shannon and Ahrens[30,31] ionic radii of hexacoordinated Mg^{2+} (0.72 Å) and Ca^{2+} (1.00 Å) cations are significantly smaller than that of Pb^{2+} (1.19 Å), whereas Ba^{2+} has a significantly larger ionic radius of 1.35 Å. In contrast, the ionic radius of Sr^{2+} (1.19 Å) is very close to that of Pb^{2+}. Therefore, we could speculate that Sr^{2+} can replace Pb^{2+} in the perovskite crystal lattice, unlike other alkaline earth metal cations. This hypothesis may explain the observed unique behavior of Sr-loaded perovskite films.

We performed a systematic analysis of a larger data set obtained for $CsPb_{0.95}M_{0.1/n}I_2Br$ films, including 30 different substituent cations. First, we plotted the absorbance at a characteristic wavelength of 630 nm for films aged for 2400 h (A_{2400}), normalized to the corresponding absorbance of the pristine films (A_0) [Figure 3(*a*)]. The A_{2400}/A_0 values were very low for about

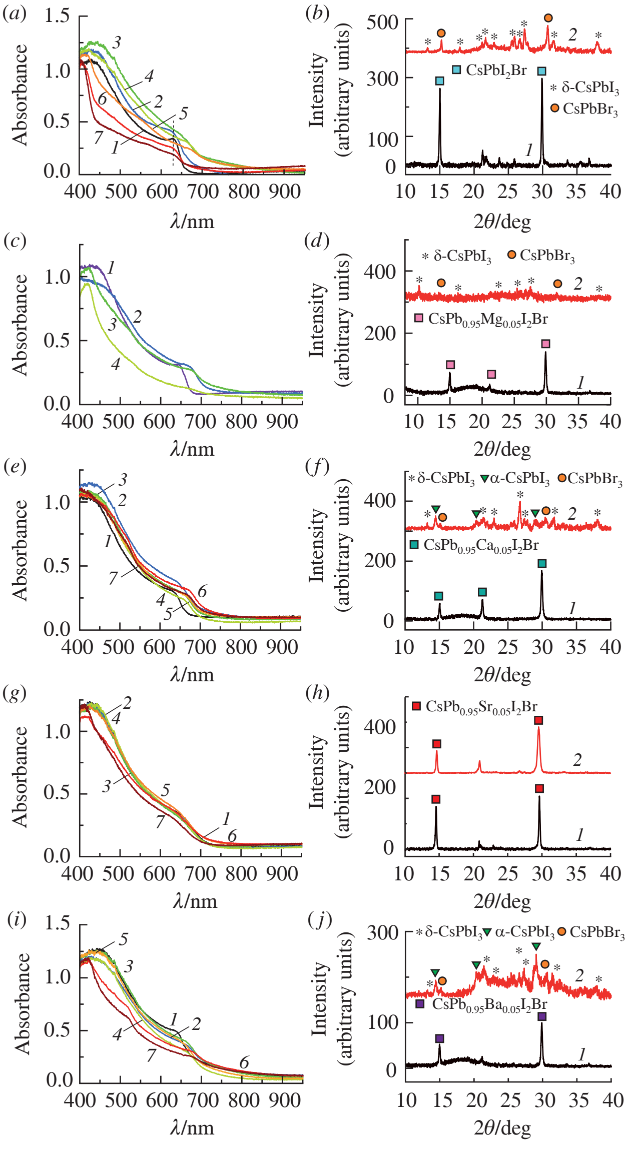

Figure 2 (*a*),(*c*),(*e*),(*g*),(*i*) Evolution of the UV-VIS absorption spectra of perovskite films after aging time (h): (*1*) 0, (*2*) 120, (*3*) 300, (*4*) 470, (*5*) 1100, (*6*) 2100 and (*7*) 2400 and (*b*),(*d*),(*f*),(*h*),(*j*) comparison of XRD patterns of (*1*) as-prepared films and (*2*) films after 2400 h aging made of perovskites (*a*),(*b*) $CsPbI_2Br$, (*c*),(*d*) $CsPb_{0.95}Mg_{0.05}I_2Br$, (*e*),(*f*) $CsPb_{0.95}Ca_{0.05}I_2Br$, (*g*),(*h*) $CsPb_{0.95}Sr_{0.05}I_2Br$ and (*i*),(*j*) $CsPb_{0.95}Ba_{0.05}I_2Br$.

---

† Precursor solutions for deposition of $CsPb_{0.95}M_{0.1/n}I_2Br$ (n is the charge number of M^{n+} cation) films were prepared by mixing 0.8 M solutions of '$CsPbI_2Br$' and '$CsM(I_{0.667}Br_{0.333})_{n+1}$' stoichiometry in dimethyl sulfoxide immediately prior to deposition of perovskite films. This methodology should be followed to prevent precipitation of solvated forms of M^{n+} halides, as we emphasized earlier.[21,22] The $CsPb_{0.95}M_{0.1/n}I_2Br$ films were obtained by spin coating of the precursor solutions at 3000 rpm directly on glass slides, followed by annealing at 150 °C for 10 min.

‡ The intrinsic photostability of the obtained films was studied under well-controlled anoxic conditions inside a nitrogen-filled glovebox using the dedicated aging test setup described earlier.[29] The films were exposed to white light with an incident light intensity of 50 mW cm^{-2} provided by metal halide lamps. Given the spectral characteristics of the light source, the samples received approximately the same number of photons as when exposed to ~80 mW cm^{-2} irradiation with the true AM1.5G solar spectrum. The sample temperature during the aging tests was in the range of 48–52 °C. The degradation of the perovskite films was monitored by periodic measurements of their UV-VIS spectra in the same glovebox without any exposure to ambient atmospheric conditions.

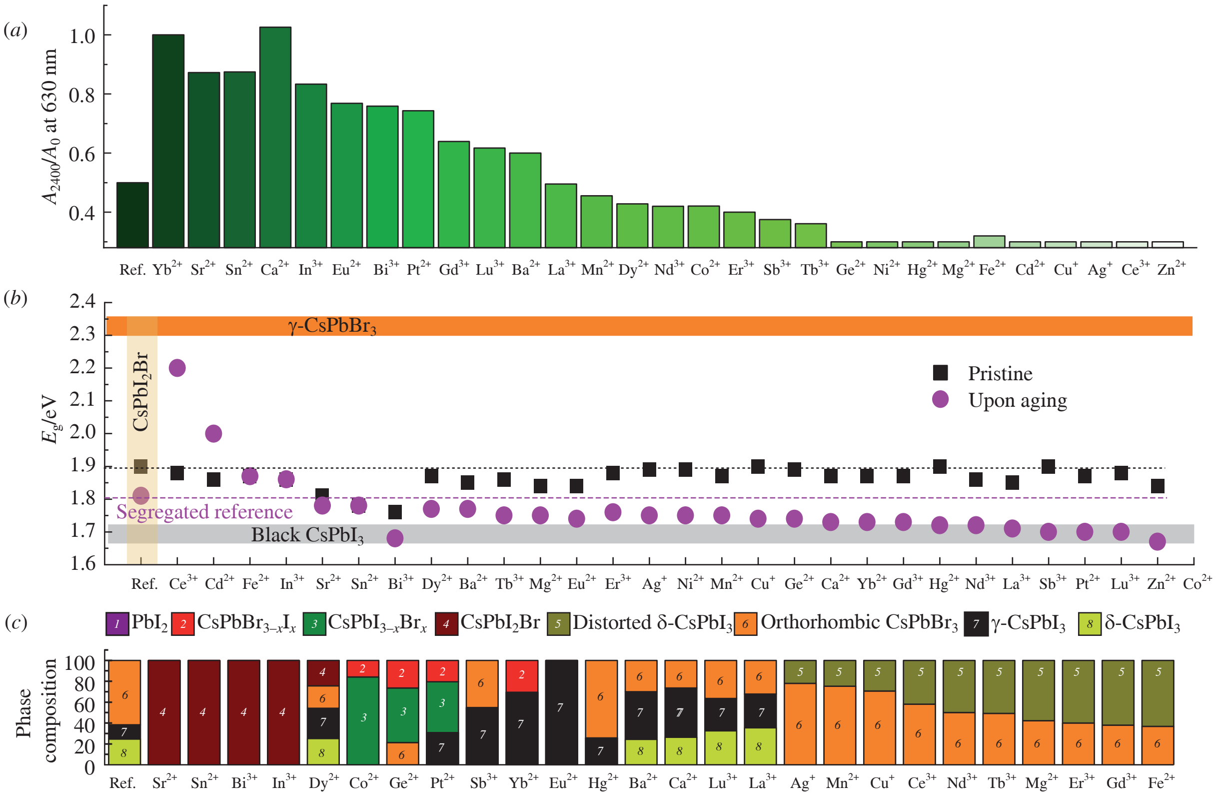

Figure 3 (*a*) Overview of the light-induced aging behavior of different $CsPb_{0.95}M_{0.1/n}I_2Br$ perovskites in terms of the normalized film absorbance A_{2400}/A_0 after 2400 h of aging. (*b*) The change of the bandgap E_g determined using the Tauc plot for the perovskites subjected to light exposure. (*c*) Phase composition of the films after 2400 h of aging according to XRD data.

half of the studied systems, indicating strong photobleaching due to segregation and further degradation of the iodide-rich perovskite phases. The most stable materials retained high A_{2400}/A_0 values in the range 0.8–1.0, although the high absorbance at 630 nm could have arisen either from the survived mixed-halide perovskite phase or from the I-rich phase that segregated but did not decompose under the aging conditions used. For example, the perovskite films modified with Yb^{2+} or Ca^{2+} exhibit the highest A_{2400}/A_0 values, while their UV-VIS spectra [Figures 2(*e*) and S2] indicate massive phase segregation and accumulation of the I-rich perovskite phase. It was previously reported that both Yb^{2+} and Ca^{2+} stabilize the black γ-phase of $CsPbI_3$, which explains why the I-rich phase remains stable after segregation from $CsPb_{0.95}Ca_{0.05}I_2Br$ and $CsPb_{0.95}Yb_{0.05}I_2Br$ films.

Another figure of merit introduced to evaluate the photostability of differently modified perovskite films is the change in their bandgap (E_g) value after long-term exposure to light [Figure 3(*b*)]. It was found that the E_g values for both $CsPb_{0.95}Ca_{0.05}I_2Br$ and $CsPb_{0.95}Yb_{0.05}I_2Br$ perovskite films evolve significantly under light soaking, indicating their instability with respect to light-induced halide phase segregation.

On the contrary, systems incorporating Fe^{2+}, Bi^{3+} or In^{3+} cations showed very small changes in E_g upon aging, similar to perovskite films modified with Sr^{2+} cations (Figures S3 and S4). Therefore, these systems have a reduced tendency to undergo light-induced halide phase segregation, although they may be unstable and degrade *via* other pathways, as observed for $CsPb_{0.95}Fe_{0.05}I_2Br$ (see Figure S3).

Finally, XRD analysis of the films subjected to light soaking for 2400 h allowed us to draw conclusions about their phase composition. Figure 3(*c*) shows that there are only very few systems in which the $CsPb_{0.95}M_{0.1/n}I_2Br$ phase survived and did not form significant amounts of I-rich (close to $CsPbI_3$) or Br-rich (similar to $CsPbBr_3$) phases. These are perovskite films incorporating Sr^{2+}, as discussed above, as well as Sn^{2+}, In^{3+} and Bi^{3+} cations. The XRD patterns of the $CsPb_{0.95}Sn_{0.05}I_2Br$ films before and after exposure to light are presented in Figure S5. The ability of Sn^{2+} to substitute Pb^{2+} in the crystal lattice is a well-recognized fact,[32] while doping of lead halide perovskites with In^{3+} and Bi^{3+} cations integrated into the crystal lattice has also been confidently supported by experimental evidence.[33,34] Thus, it can be assumed that the light-induced segregation of the halide phase in mixed-halide perovskite films could be suppressed by metal cations capable of being integrated into the perovskite crystal lattice.

In summary, we have performed a systematic study of a large series of $CsPb_{0.95}M_{0.1/n}I_2Br$ systems incorporating 30 different substituent M^{n+} cations. It has been shown that the light-induced phase segregation of these materials with the formation of iodide-rich and bromide-rich phases could be effectively suppressed by appropriate compositional engineering. The Sr^{2+}, Sn^{2+}, In^{3+} and Bi^{3+} cations were particularly effective in blocking the photodegradation of the corresponding perovskite films, and this behavior correlates with the ability of these cations to substitute Pb^{2+} in the perovskite crystal lattice. This hypothesis requires future verification and careful mechanistic analysis, since the observed effect may be of great fundamental importance. The obtained results, however, seem to be very promising from a practical point of view, as they pave the way for the development of photostable wide-bandgap mixed-halide perovskite absorber materials, which are essential for tandem photovoltaic applications using low-bandgap Si or CIGS subcells.[35]

This work was supported by the Ministry of Science and Higher Education of the Russian Federation [grant no. 075-15-2022-1217 (13.2251.21.0163)].

Online Supplementary Materials

Supplementary data associated with this article can be found in the online version at doi: 10.71267/mencom.7698.

References

1 G. Wang, J. Chang, J. Bi, W. Zhang and F. Meng, *Sol. RRL*, 2022, **6**, 2200656; https://doi.org/10.1002/solr.202200656.

2 B. Wang, X. Yin, S. Iqbal, M. Que and W. Que, *Adv. Mater. Interfaces*, 2022, **9**, 2200636; https://doi.org/10.1002/admi.202200636.

3 X.-Y. Li, Q. Sun, Y.-M. Xie and M.-K. Fung, *Adv. Energy Sustainability Res.*, 2024, **5**, 2300263; https://doi.org/10.1002/aesr.202300263.

4 H. J. Lee, J. H. Heo and S. H. Im, *Appl. Phys. Rev.*, 2024, **11**, 031301; https://doi.org/10.1063/5.0202332.

5 J. Wang, G. Wang and B. Chen, *Sustainable Energy Fuels*, 2024, **8**, 4667; https://doi.org/10.1039/D4SE00914B.

6 H. Jin, Y.-J. Zeng, J. A. Steele, M. B. J. Roeffaers, J. Hofkens and E. Debroye, *NPG Asia Mater.*, 2024, **16**, 24; https://doi.org/10.1038/s41427-024-00540-0.

7 N. N. Dremova, G. V. Shilov, P. A. Troshin and L. A. Frolova, *Mendeleev Commun.*, 2024, **34**, 481; https://doi.org/10.1016/j.mencom.2024.06.004.

8 Y. Guo, H. Liu, W. Li, L. Zhu and H. Chen, *Sol. RRL*, 2020, **4**, 2000380; https://doi.org/10.1002/solr.202000380.

9 E. L. Lim, J. Yang and Z. Wei, *Energy Environ. Sci.*, 2023, **16**, 862; https://doi.org/10.1039/D2EE03539A.

10 X. Liu, J. Li, X. Cui, X. Wang and D. Yang, *J. Mater. Chem. C*, 2023, **11**, 426; https://doi.org/10.1039/D2TC03631B.

11 J. Song, H. Xie, E. L. Lim, A. Hagfeldt and D. Bi, *Adv. Energy Mater.*, 2022, **12**, 2201854; https://doi.org/10.1002/aenm.202201854.

12 X. Li, J. Tang, P. Zhang and S. Li, *Cell Rep. Phys. Sci.*, 2024, **5**, 101842; https://doi.org/10.1016/j.xcrp.2024.101842.

13 Z. Cheng, M. Zhang, Y. Zhang, W. Qi, Z. Wang, B. Liu and D. Di, *Nano Energy*, 2024, **127**, 109708; https://doi.org/10.1016/j.nanoen.2024.109708.

14 L. A. Frolova, S. Y. Luchkin, Y. Lekina, L. G. Gutsev, S. A. Tsarev, I. S. Zhidkov, E. Z. Kurmaev, Z. X. Shen, K. J. Stevenson, S. M. Aldoshin and P. A. Troshin, *Adv. Energy Mater.*, 2021, **11**, 2002934; https://doi.org/10.1002/aenm.202002934.

15 L. A. Frolova, Q. Chang, S. Yu. Luchkin, D. Zhao, A. F. Akbulatov, N. N. Dremova, A. V. Ivanov, E. E. M. Chia, K. J. Stevenson and P. A. Troshin, *J. Mater. Chem. C*, 2019, **7**, 5314; https://doi.org/10.1039/C8TC04488K.

16 M. He, C. Xing, Q. Bao, L. Yu, Z. Nie, R. Wang, C. Wan, D. Wang and T. Zhang, *ACS Appl. Mater. Interfaces*, 2024, **16**, 62392; https://doi.org/10.1021/acsami.4c13643.

17 D. Wang, Z. Nie, F. Lu, C. Xing, Q. Bao, M. He and T. Zhang, *ACS Appl. Energy Mater.*, 2024, **7**, 9483; https://doi.org/10.1021/acsaem.4c02149.

18 L. He, M. Zhong, Y. Jiang, L. Shang and Y. Gao, *Mater. Today Commun.*, 2024, **39**, 109282; https://doi.org/10.1016/j.mtcomm.2024.109282.

19 M. K. Kuznetsov, N. A. Emelianov, D. V. Korchagin, G. V. Shilov, S. M. Aldoshin, P. A. Troshin and L. A. Frolova, *Sustainable Energy Fuels*, 2022, **6**, 3536; https://doi.org/10.1039/D2SE00450J.

20 L. A. Frolova, D. V. Anokhin, K. L. Gerasimov, N. N. Dremova and P. A. Troshin, *J. Phys. Chem. Lett.*, 2016, **7**, 4353; https://doi.org/10.1021/acs.jpclett.6b02122.

21 M. I. Ustinova, M. M. Mikheeva, G. V. Shilov, N. N. Dremova, L. Frolova, K. J. Stevenson, S. M. Aldoshin and P. A. Troshin, *ACS Appl. Mater. Interfaces*, 2021, **13**, 5184; https://doi.org/10.1021/acsami.0c18061.

22 M. I. Ustinova, M. V. Lobanov, G. V. Shilov, N. N. Dremova, A. F. Akbulatov, L. G. Gutsev, I. S. Zhidkov, E. Z. Kurmaev, F. A. Prudnov, A. V. Ivanov, L. A. Frolova, S. M. Aldoshin and P. A. Troshin, *Adv. Funct. Mater.*, 2025, **35**, 2407571; https://doi.org/10.1002/adfm.202407571.

23 W. Li, H. Tong, Y. Li, X. Liu, G. Wan, X. Ma, H. Liu, Z. Gao, Y. Fu, D. He, Z. Li and J. Li, *Small*, 2024, **20**, 2406784; https://doi.org/10.1002/smll.202406784.

24 P. Ma, T. Bie, Y. Liu, L. Yang, S. Bi, Z. Wang and M. Shao, *ACS Appl. Mater. Interfaces*, 2024, **16**, 1217; https://doi.org/10.1021/acsami.3c14459.

25 S. R. Rondiya, S. S. Mali, A. Roy, G. K. Inwati, G. K. Rahane, Y. A. Jadhav, S. Suresh, T. Debnath, C. K. Hong and N. Y. Dzade, *Phys. Chem. Chem. Phys.*, 2023, **25**, 29050; https://doi.org/10.1039/d3cp02935b.

26 C. F. J. Lau, M. Zhang, X. Deng, J. Zheng, J. Bing, Q. Ma, J. Kim, L. Hu, M. A. Green, S. Huang and A. Ho-Baillie, *ACS Energy Lett.*, 2017, **2**, 2319; https://doi.org/10.1021/acsenergylett.7b00751.

27 Z. Guo, S. Zhao, A. Liu, Y. Kamata, S. Teo, S. Yang, Z. Xu, S. Hayase and T. Ma, *ACS Appl. Mater. Interfaces*, 2019, **11**, 19994; https://doi.org/10.1021/acsami.9b03622.

28 W. Xiang, Z. Wang, D. J. Kubicki, W. Tress, J. Luo, D. Prochowicz, S. Akin, L. Emsley, J. Zhou, G. Dietler, M. Grätzel and A. Hagfeldt, *Joule*, 2019, **3**, 205; https://doi.org/10.1016/j.joule.2018.10.008.

29 A. F. Akbulatov, M. I. Ustinova, L. Gutsev, S. A. Tsarev, N. N. Dremova, I. Zhidkov, S. Yu. Luchkin, B. R. Ramachandran, L. Frolova, E. Z. Kurmaev, K. J. Stevenson, S. M. Aldoshin and P. A. Troshin, *Nano Energy*, 2021, **86**, 106082; https://doi.org/10.1016/j.nanoen.2021.106082.

30 R. D. Shannon, *Acta Crystallogr., Sect. A: Cryst. Phys., Diffr., Theor. Gen. Crystallogr.*, 1976, **32**, 751; https://doi.org/10.1107/S0567739476001551.

31 L. H. Ahrens, *Geochim. Cosmochim. Acta*, 1952, **2**, 155; https://doi.org/10.1016/0016-7037(52)90004-5.

32 T. Liu, X. Zhao, X. Zhong, Q. C. Burlingame, A. Kahn and Y.-L. Loo, *ACS Energy Lett.*, 2022, **7**, 3531; https://doi.org/10.1021/acsenergylett.2c01610.

33 R. Meng, G. Wu, J. Zhou, H. Zhou, H. Fang, M. A. Loi and Y. Zhang, *Chem. – Eur. J.*, 2019, **25**, 5480; https://doi.org/10.1002/chem.201805370.

34 C. Liu, W. Li, H. Li, H. Wang, C. Zhang, Y. Yang, X. Gao, Q. Xue, H.-L. Yip, J. Fan, R. E. I. Schropp and Y. Mai, *Adv. Energy Mater.*, 2019, **9**, 1803572; https://doi.org/10.1002/aenm.201803572.

35 J. Liu, Y. He, L. Ding, H. Zhang, Q. Li, L. Jia, J. Yu, T. W. Lau, M. Li, Y. Qin, X. Gu, F. Zhang, Q. Li, Y. Yang, S. Zhao, X. Wu, J. Liu, T. Liu, Y. Gao, Y. Wang, X. Dong, H. Chen, P. Li, T. Zhou, M. Yang, X. Ru, F. Peng, S. Yin, M. Qu, D. Zhao, Z. Zhao, M. Li, P. Guo, H. Yan, C. Xiao, P. Xiao, J. Yin, X. Zhang, Z. Li, B. He and X. Xu, *Nature*, 2024, **635**, 596; https://doi.org/10.1038/s41586-024-07997-7.

Received: 2nd December 2024; Com. 24/7698